Journal of Engg. Research Vol. 7 No. (2) June 2019 pp. 259-280

A new approach for the fault identification, localization, and classification in the power system

Nejra Čišija-Kobilica*, Samir Avdaković**, Jasna Hivziefendić* and Armin Kobilica***

*Department of Electrical and Electronics Engineering, International Burch University, Sarajevo, Bosnia and Herzegovina
Specialty of Signal Analysis; jasna.hivziefendic@ibu.edu.ba Specialty of Planning Distribution Network
**Faculty of Electrical Engineering, University of Sarajevo, Bosnia and Herzegovina, samir.avdakovic@etf.unsa.ba
***Information and Computer Science Department, King Fahd University of Petroleum and Minerals, Dhahran, Saudi Arabia, g201403920@kfupm.edu.sa Specialty of Machine Learning
*Corresponding Author: nejra.cisija@ibu.edu.ba

ABSTRACT

The recent structure of the monitoring, protection, and control of the power systems includes GPS timely synchronized measurement units (Phasor Measurement Units). With the implementation of these units, Wide-Area Monitoring, Protection and Control Systems are required to perform fast and efficient identification of the disturbances that may lead to cascade propagation and blackouts in the power system. The requirements furthermore enable appropriate actions, preventive and corrective measures to minimize effects of the occurring disturbances. This paper proposes the application of the discrete Teager Energy Operator for the power system fault identification, localization, and classification. Identification and localization of the disturbances are performed with the analysis of available signals with the application of the Teager Energy Operator and comparison of its peak values at several points in the system. The proposed classifier of the disturbances is based on the Teager Energy Operator analysis of available signals and values of df/dt indicator of active power unbalance at several points in the system. Simulations are performed in the New England 39 bus test system using DIgSILENT Power Factory software. The performance and the comparison of the applied techniques are assessed through a large number of the simulated faults for the specific fault type. Fault identification and localization results are compared with the results obtained in the analysis performed with Discrete Wavelet Transform and Hilbert-Huang Transform indicating on satisfactory performance of the proposed approach. Furthermore, the proposed approach provides notable results in the fault classification performed according to 141 simulated faults. Teager Energy Operator in the proposed method outperforms other techniques with less computational work and faster estimation, enabling the development of a relatively simple algorithm for the fast and efficient identification, localization, and classification of the disturbances in power system.

Keywords: Artificial neural network; Fault detection; Power system dynamics; Teager Energy Operator.

INTRODUCTION

Disturbances in the power systems can be caused by different phenomena (transient instabilities, voltage instabilities, overloads, etc.). Overload of the power system elements can have cascading effects on the other elements, particularly transmission lines, and, eventually, it can cause total system blackout (Grigsby, 2007). Faults that occur on these lines may threaten the system stability since transmission lines enable power transfer from the generators to the consumers (Reddy et al., 2014). The motivation for eventual prevention of these catastrophic failures made the concept of smart grid present all over the world. A key component for the development of the smart power transmission systems is the implementation of Wide-Area Monitoring, Protection and Control Systems (WAMPAC). These systems are based on the synchronized measurements from the phasor measurement units (PMUs). Multiple PMUs are placed at several positions in the power system as a complement to the conventional measurements (Muller et al., 2012). The whole WAMS (Wide Area Measurement System) is monitored with a required number of PMUs that are 1/5-1/4 of all buses in the system (Lee et al., 2016). PMUs measure and record real power system data. Processing of a large amount of synchronized data, for the purpose of fault features extraction, is a challenge for the fault location task (Zhang et al., 2012). Power system operation is expected to be maintained by processing WAMS data online with a wide range of the developed algorithms (Wall et al., 2016). The current effort is dedicated to developing mechanisms that will use these data to provide appropriate information to the power system operators in order to timely respond against blackouts. Next to this development, important improvement in data analysis methods is achieved (Chakrabortty et al., 2013). With appropriate signal processing technique, WAMS enables identification and localization of the disturbances. The fault detection task will be possible to perform with the process of receiving data from the WAMPAC systems.

Wavelet Transform is considered as a useful tool in the analysis of non-stationary signals. Neto et al. (2013) have used it for the real-time detection of high-frequency electrical oscillations and low-frequency electromechanical oscillations (LFEO) for synchronous generator fault situations. LFEO are identified with scaling coefficient energy extracted from the active power while wavelet coefficient energy enables identification of high-frequency electrical oscillations. Fault detection is performed through an increase in energy. The presented algorithm in Neto et al. (2013) is tested in an experimental grid with different mother wavelets used. Analysis based on wavelet transform depends on the mother wavelet type and the number of the decomposition levels. Choosing appropriate mother wavelet is an important task in the fault detection with wavelet transform. Results obtained with different types of the mother wavelets may differ a lot. An increment in the number of the decomposition levels will extend the filtering processes that can also affect achieved results (Neto et al., 2013).

In (Messina, 2009), it is highlighted that, for the estimation of the power systems electromechanical modal properties, time-synchronized measurements (data) provide rich information. One of the challenging tasks in data processing is a spectral analysis of the power system oscillatory signal data. A technique that overcomes the disadvantage of the finite time window, Hilbert-Huang Technique (HHT), is proposed in (Messina, 2009).

The main advantage of the proposed TEO application is its simple theoretical background that provides a straight approach in the signal analysis. In this paper, the area of the Teager Energy Operator application is expanded to the area of the power systems fault identification, localization, and classification (in the area of frequency range up to 5 Hz). The contributions achieved in this work can be summarized as follows:

- Application of the TEO for the complete fault detection process (identification, localization, and classification) based on the analysis of the available PMUs signals,
- Notable results achieved with less computational work and faster estimation using TEO for signal processing, in comparison with DWT and HHT,
- The proposed classifier of the disturbances, based on the application of the DWT and TEO extracted features as compound input to the designed ANN.

The rest of the paper is organized as follows. Section 2 gives a review of the literature related to the application of the Teager Energy Operator in the power system. In Section 3, a short mathematical description of used signal processing techniques is given. Proposed approach in terms of the performed analysis is presented in Section 4. Section 5 shows the obtained results with adequate discussion made. Complete work is concluded in Section 6.

APPLICATION OF TEO IN THE POWER SYSTEM

Different applications of TEO in the power system during the last period are presented below. In the selected papers, TEO is used for power quality problems, oscillation problems, and fault detection, amplitude, and frequency estimation. Papers are listed in descending order according to year of publishing.

Identification of LFEO is performed in (Xiao et al., 2017) with the application of variational mode decomposition (VMD) and TEO. Signals are decomposed using VMD into several components represented as a set of limited bandwidths with the center frequency. The amplitude, frequency, and damping factor of each component are determined with TEO. The validation of the proposed method is performed through the IEEE two-area four-generator test system and New England (NE) 39-bus system. The good performance is achieved in oscillation mode extraction.

The estimation of the voltage flicker components using improved Teager Energy Operator (ITEO) is presented in (Li et al., 2016). The envelope components of voltage flicker are extracted by ITEO. Proposed approach reduces the computation and overcomes harmonics and interharmonics. Further, this approach overcomes fluctuation of the fundamental frequency and white noise. With the simulation and experimental application, the proposed method provides accurate and efficient results (Li et al., 2016).

It is stated in (Kumar et al., 2016) that Teager energy was initially used for AM-FM demodulation and to estimate the envelope of the amplitude of AM signals with application related to the AM-FM energy detection, noise separation, and speech signals analysis. In (Kumar et al., 2016), the algorithm for the detection of the faults during power swing based on TEO is proposed.

Detection and classification of power quality (PQ) disturbance using TEO are performed in (Chen et al., 2016). Features are extracted with the application of mathematical morphology (MM) and TEO. MM operators extract transient features while TEO extracts energy feature from the disturbance signals. Classification is obtained with PNN. Obtained results highlight that the presented approach can accurately perform detection and classification of the simulated disturbances.

Teager Energy using Empirical Mode Decomposition (EMD) and HHT is estimated in (Ramakrishna et al., 2016). It is preferred in applications due to the simplicity of this operator and its robustness to the noisy environment. In the Teager Huang Transform (THT), signals are decomposed into Intrinsic Mode Functions (IMFs). IMFs are then used in Discrete Energy Separation Algorithm (DESA) for estimation of the instantaneous amplitudes and frequencies.

TEO is used in (Hasheminejad et al., 2016) for parallel transmission lines protection in order to achieve the identification, location, and classification of transmission line faults. Fault situation can be indicated by the peak of the Teager energy value. The proposed algorithm is tested on various generated internal faults. Achieved results show that this algorithm is a suitable algorithm for the correct and fast identification and classification of all performed tests (Hasheminejad et al., 2016). Presented work is completed in (Hasheminejad et al., 2017) with the identification and classification of phase-to-phase and phase-to-phase to ground inter-circuit fault. Current traveling waves (TW) are extracted with TEO. Since TEO reflects changes in the signal amplitude, a peak in the TEO output represents a TW. The proposed algorithm is tested on a large number of input signals and accomplished the accurate performance.

Measurement of the power system harmonics, as one of the power quality problems, is performed in (Yao et al., 2016). Harmonic signals are decomposed with linear filter bank in order to eliminate the mutual influence between harmonic components. The change of each harmonic component is tracked with the application of Teager-Kaiser Energy Operator. The proposed method is tested with the simulation and practical experiments, achieving high accuracy measurements.

An algorithm based on TEO in (Yin et al, 2015) determines whether the rotor bars in the induction motor are broken or not, by analyzing one phase current signal.

In (Reza et al., 2015), fundamental frequency of a phase voltage is estimated under different system conditions. Applied technique combines the TEO and frequency adaptive bandpass filter (BPF) to estimate the fundamental frequency and extract the normalized amplitude of the grid voltage fundamental component. The technique is tested in the simulation and experimental study and analyzed in detail. Obtained results indicate the effective application of the technique.

Authors in (Hongbo et al., 2014) highlighted attraction for the fast and accurate voltage estimation in the presence of harmonic distortion. Instantaneous amplitude and frequency can be identified by TEO. The energy separation algorithm (ESA) provided better time resolution in comparison with the Hilbert Transform. In (Maragos et al., 1993), AM-FM signal demodulation is achieved with separation of a signal into its amplitude $|a(t)|$ and the instantaneous frequency signal $f(t)$ with ESA using TEO. In this paper, the authors showed that the presented algorithm can track the variable amplitude of the fundamental of the power signal (Hongbo et al., 2014).

IEEE 39 bus system is analyzed by (Zhang et al., 2012) for the verification of the fault detection method based on the Bayesian discriminant analysis rule. The proposed method gave accurate and reliable results.

In (Kamwa et al., 2011), Teager-Kaiser energy operator (TKEO) is used as a predictor of power oscillation problems with author's indication that this is the first time of TKEO application in this context. Multi-band prefiltering is firstly performed in order to overcome poor performance of this concept on multi-component signals (Maragos et al., 1993). ESA is then conducted with the filtered signal. The Eigen system realization algorithm (ERA) form is used for improving frequency resolution and providing damping information. Instantaneous amplitude and frequency are estimated with TKEO application to the output signals of a linear filter bank. Artificial modes are possible to occur in instantaneous amplitude and frequency estimation with empirical mode decomposition implementation. The proposed algorithm is tested with the analysis of a real unstable situation registered in the Hydro-Quebec WAMS, giving an indication of real-life oscillation problems successful detection (Kamwa et al., 2011).

Related papers justify application of the TEO for the purpose of the fault identification and fault localization.

The power system is constantly exposed to the different disturbances. Disturbances can be different in the type and different in the intensity. Load changes continually exist as small disturbances, and system operation under these changes needs to be satisfactory and handle load demand. It needs to handle many different disturbances, e.g., short circuit on a transmission line or loss of a large generator (Grigsby, 2007). Some of the disturbances can lead system to the partial or total blackout. Monitoring of the power system oscillations is important in the prevention of the widespread blackouts. The frequency range of the LFEO is 0.1-2 Hz (Rueda et al., 2011). The range can be related to the local modes (1-2 Hz) or interarea modes (0.1-1 Hz). Local modes are related to the generation units swinging with respect to the rest of the power system while interarea modes are related with many machines swinging in one part of the system against machines in other parts (Prasertwong et al., 2010). Some disturbances that can potentially cause LFEO are generator outage (GO), transmission line outage (TLO), and short-circuit (SC). These fault types with the addition of short circuit followed by transmission line outage are simulated in this paper through numerous simulations at different locations in the system. Presence of accurate fault detection methodologies is essential to the restoration of the system after the fault occurred (Reddy et al., 2014).

SIGNAL PROCESSING TECHNIQUES

Different signal processing techniques have been proposed in the power system fault detection until now. DWT, HHT, and TEO are applied and compared in this paper. Theoretical background of the applied techniques is given below.

Teager Energy Operator

A simple algorithm based on Teager Energy Operator is used for extracting energy properties of the signal that has been analyzed. If the signal is in the form

$$x(n) = A\cos(\Omega n + \phi), \tag{1}$$

the above expression is used in

$$\psi[x(n)] = x^2(n) - x(n-1)x(n+1) \approx A^2\Omega^2. \tag{2}$$

This is the formulation of a Teager algorithm for obtaining a measure of the energy in a single-component signal. The operator uses only three successive samples of the signal. Application of the algorithm to the multi-frequency component signals does not give the energy of the system that generates those signals. However, when the multi-component signal is at its peak, output of the algorithm is maximum, and it is minimum when the signal is at zero (Kaiser, 1990).

Instantaneous amplitude and frequency of the signal can be determined with the application of this operator in the energy separation algorithm (ESA) (Chen et al., 2016 & Hongbo et al., 2014).

Discrete Wavelet Transform

The Wavelet Transform provides the separation of the signals into different frequency components in terms of the different frequency ranges.

The base for the transform is mother wavelet ψ - function with zero average. Wavelets $(\psi_{m,n})$ are formed by scaling (scale parameter a) and shifting (translation parameter b) of the mother wavelet ψ. Good time-frequency localization properties are obtained with $a_0 = 2$ and $b_0 = 2$ (Daubechies, 1992).

Parameters a and b take only discrete values for the DWT that is obtained by the convolution of the discrete signal $x(t)$ with wavelet $\psi_{m,n}$ (Mallat, 1998).

$$DWT(x,m,n) = \int_{-\infty}^{\infty} x(t)\psi_{m,n}^{*}(t)dt. \tag{3}$$

Hilbert-Huang Transform

EMD decomposes an original signal into IMFs. HHT is then applied to the obtained IMFs. Hilbert-Huang Transform $y(t)$ of the signal $x(t)$ is given by

$$y(t) = \frac{1}{\pi}\int_{-\infty}^{\infty} \frac{x(\tau)}{t-\tau}d\tau. \tag{4}$$

In the next expressions, $a(t)$ is the amplitude and $\theta(t)$ is a phase of the analytic signal $z(t)$ computed as

$$a(t) = \sqrt{x^2(t) + y^2(t),} \tag{5}$$

$$\theta(t) = arctan\frac{y(t)}{x(t)}. \tag{6}$$

Signal $z(t)$ indicates on signal $x(t)$ locality where the instantaneous frequency is determined (Hayes et al., 2016)

$$\omega(t) = \frac{d\theta(t)}{dt}. \tag{7}$$

OVERVIEW OF THE PERFORMED ANALYSIS

As illustration example, signals obtained from the simulation of the transmission line outage (TLO) fault type are analyzed in this section. The signal analysis is performed with DWT, HHT, and TEO. The same analysis process is conducted for all faults simulated in this work (Fig. 1).

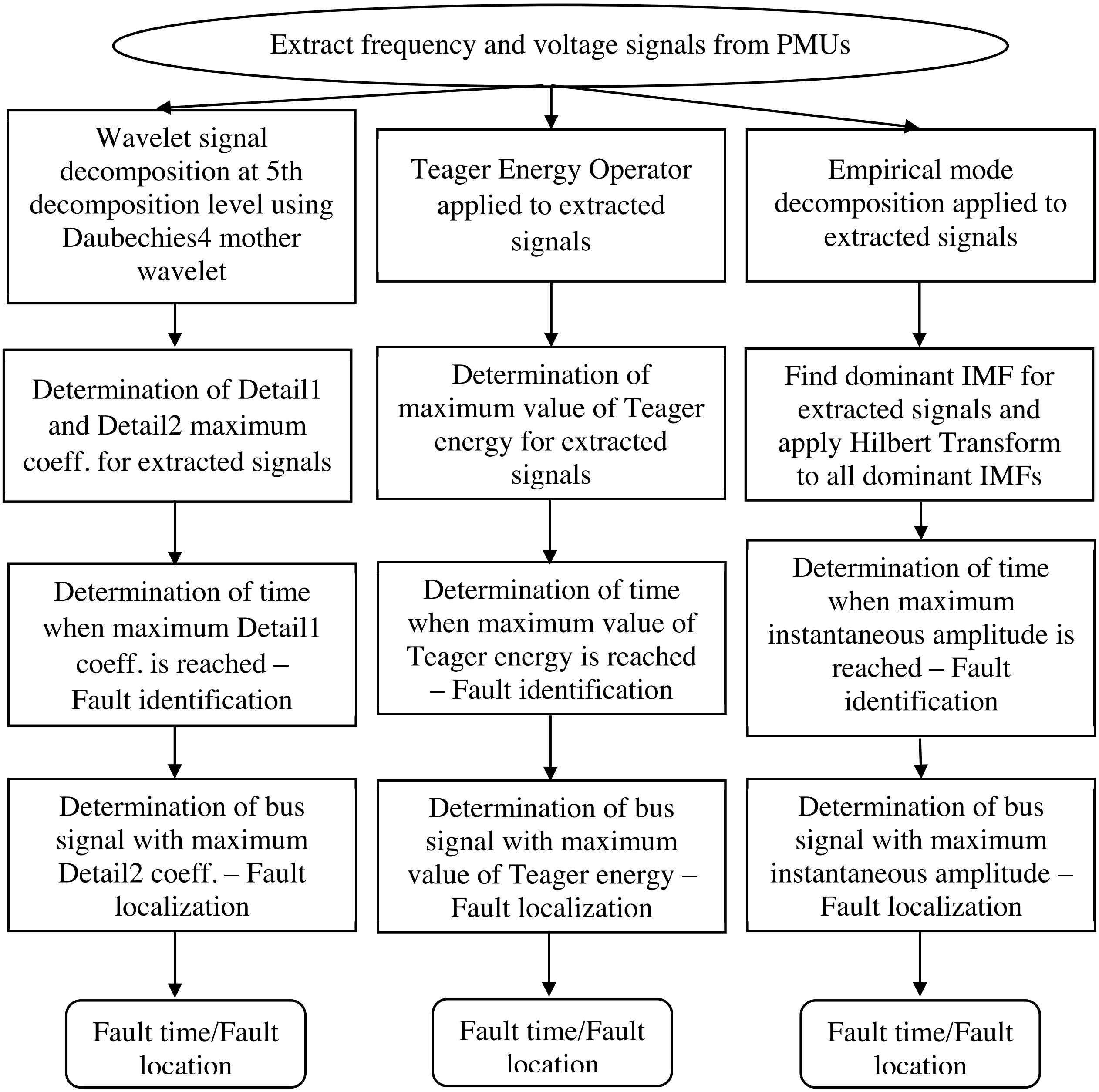

Fig. 1. Proposed approach for the fault identification and localization.

Faults are simulated in NE 39-bus test system (Fig. 2). Results of the optimal placement of PMUs are taken from (Ivatloo, 2009). Frequency and voltage signals are therefore obtained from the buses 2, 6, 9, 10, 11, 14, 17, 19, 20, 22, 23, 25, and 29 (Fig. 2) that correspond to the appropriate PMUs positions.

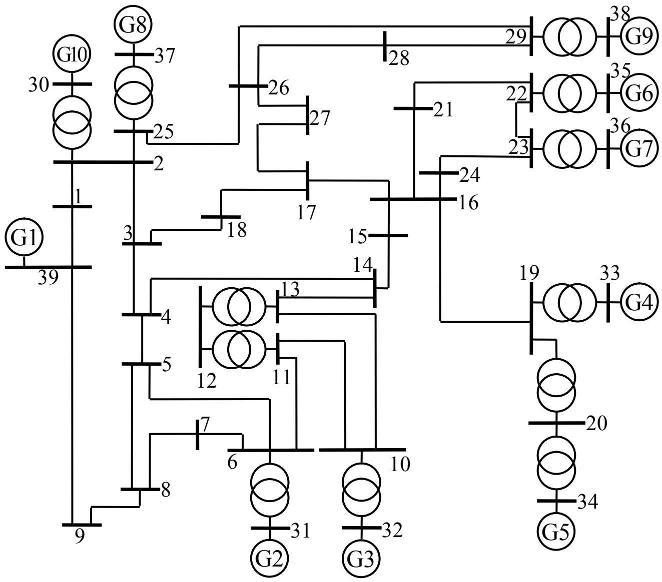

Fig. 2. NE 39 bus test system (Avdakovic et al., 2014).

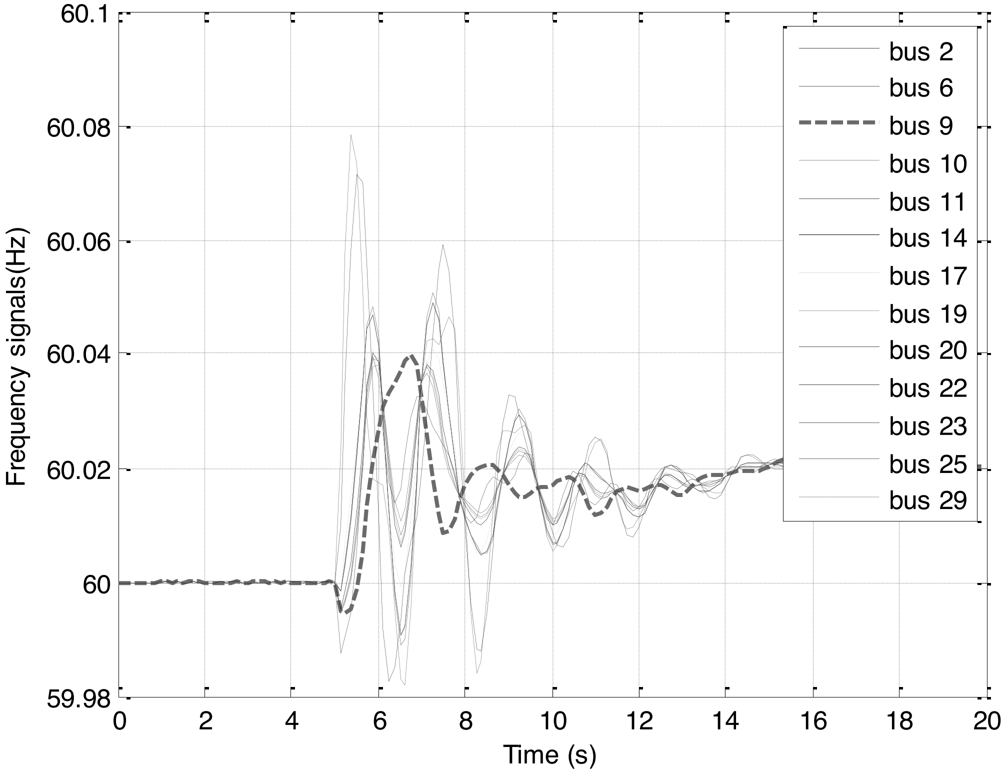

Fig. 3. Frequency signals for the transmission lines 2-25 outage.

An outage of the transmission line between buses 2 and 25 is simulated at 5th second. Obtained frequency signals are presented in Fig. 3. Identification and localization of this fault are performed by the analysis of the frequency signals with DWT, HHT, and TEO techniques.

Simulations are made by sampling frequency f_s of 8Hz, making time step of 0.125s. According to the Nyquist sampling theory, the frequency that can be contained and analyzed in the signals is in the range 0-4 Hz, and that is sufficient for analyzing LFEO. DWT signal decomposition is performed to 5th decomposition level since further decompositions will extract very low frequencies (less than 0.125 Hz), not observed in this study.

There are different wavelet families established until now and in each family different wavelets implementations. The most known family is Daubechies filters. Mother wavelet Daubechies 4 (db4) is used in this work as a base for the performed wavelet transform since it is successfully applied for the detection of the LFEO in (Avdaković et al., 2012).

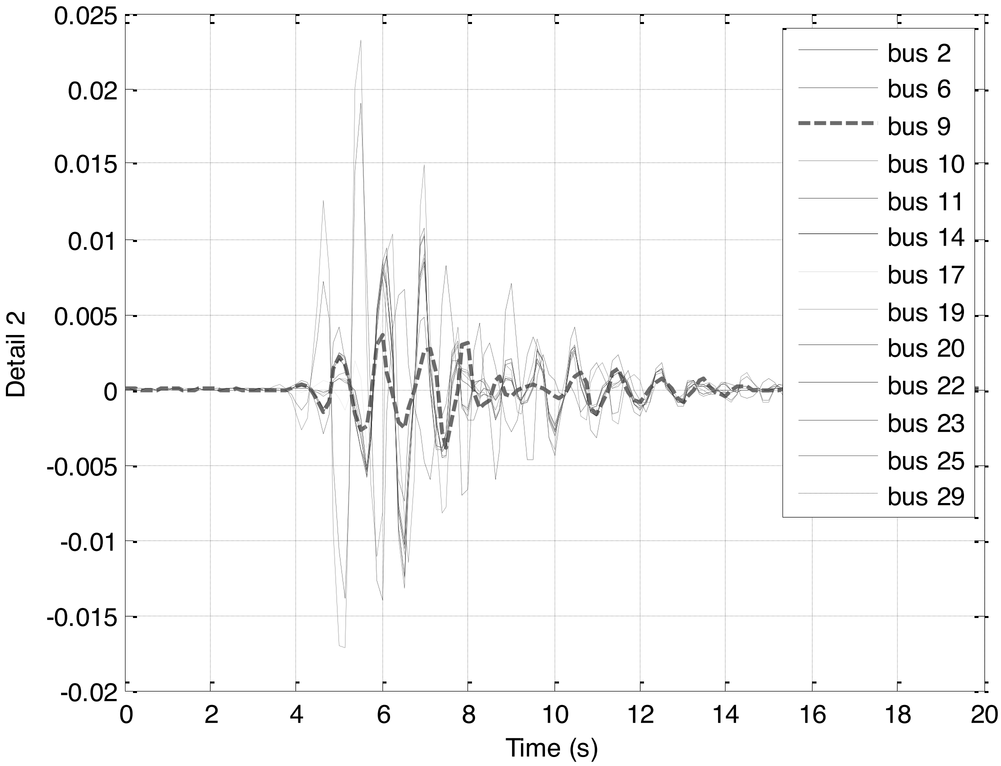

Fig. 4. Detail 2 of frequency signals for the transmission lines 2-25 outage.

Signals are processed with DWT in two steps. The original discrete signal is split into two separate signals (approximation and detail coefficients) with low pass and high pass filters (LPF and HPF) – first level. The first level of the signal decomposition is used for the identification of the event. Detail coefficients of the first level (Detail 1) are extracted for the identification part of the analysis since they will detect any change in the signal (nature of the fault). The range of the frequencies is 2-4 Hz. After that signal filtration is performed again, in a way that approximation coefficients of the first level are filtered with LPF and HPF; this gives approximation and detail coefficients of the second level. Frequencies of detail coefficients of the second level (Detail 2) are in the range 1-2 Hz. Amplitudes of Detail 2 are used for the fault localization, detecting local mode oscillations. Thus, fault time is defined by analysis of Detail 1 and fault location is defined with analysis of Detail 2. As can be noticed from Fig. 4, frequency signal from bus 25 (marked red in the graph) has a maximum value of Detail 2 from all 13 signals. Therefore, bus 25 is marked as fault location, which makes this fault localization the correct one. The maximum value of Detail 1 is reached at 5.25 seconds what is marked as fault time (Fig. 5).

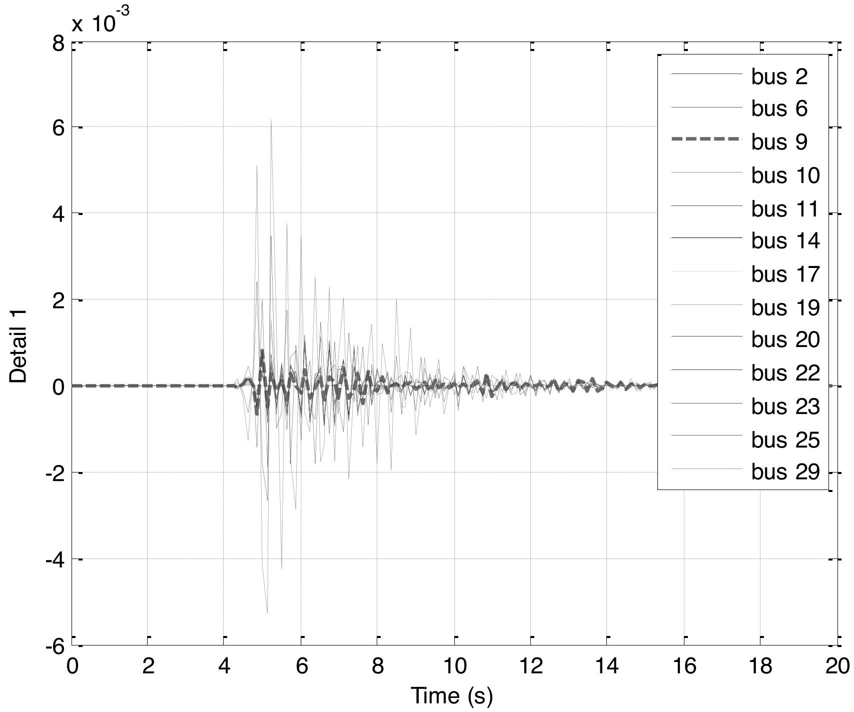

Fig. 5. Detail 1 of frequency signals for the transmission lines 2-25 outage.

Signals are also analyzed with HHT. Empirical mode decomposition (EMD) is performed on all 13 signals and dominant IMF for each signal is determined (Fig. 6). Dominant IMF is determined as IMF with the highest value of standard deviation (Hayes e t al., 2016).

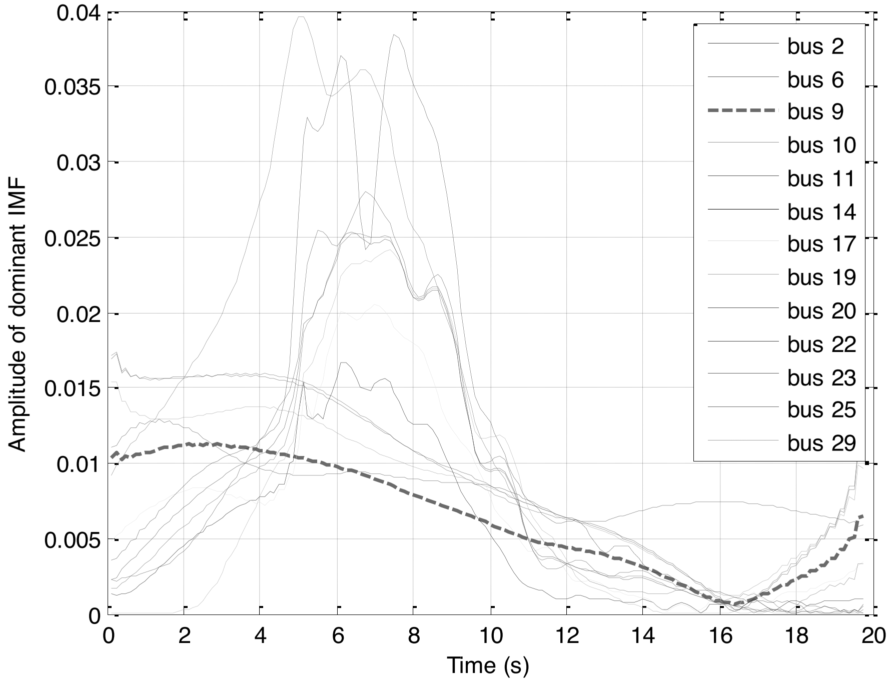

Fig. 6. Amplitudes of dominant IMFs.

Maximum amplitude is reached for the dominant IMF of the frequency signal from bus 25 (marked red in Fig. 6) at 5 seconds. Thus, bus 25 is marked as fault location and time of 5 seconds as fault time. Dominant IMF for the frequency signal from bus 25 is the second IMF (Fig. 7).

TEO is applied to the same signals as well (Fig. 8). Maximum TE (Teager Energy) is obtained for the case of the frequency signal from bus 25 (marked red in the graph) at 5.375 seconds.

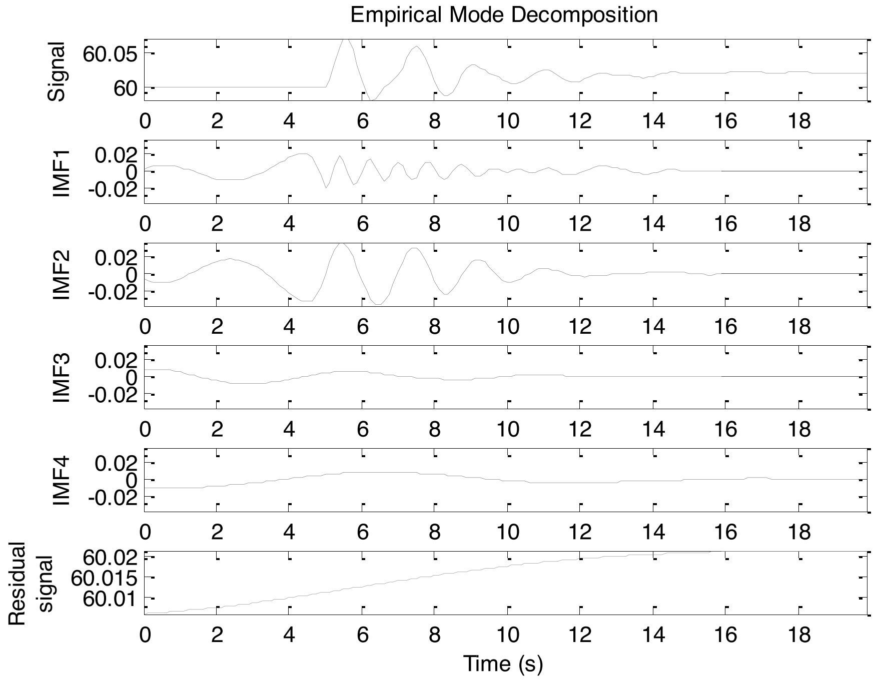

Fig. 7. EMD of the frequency signal from bus 25.

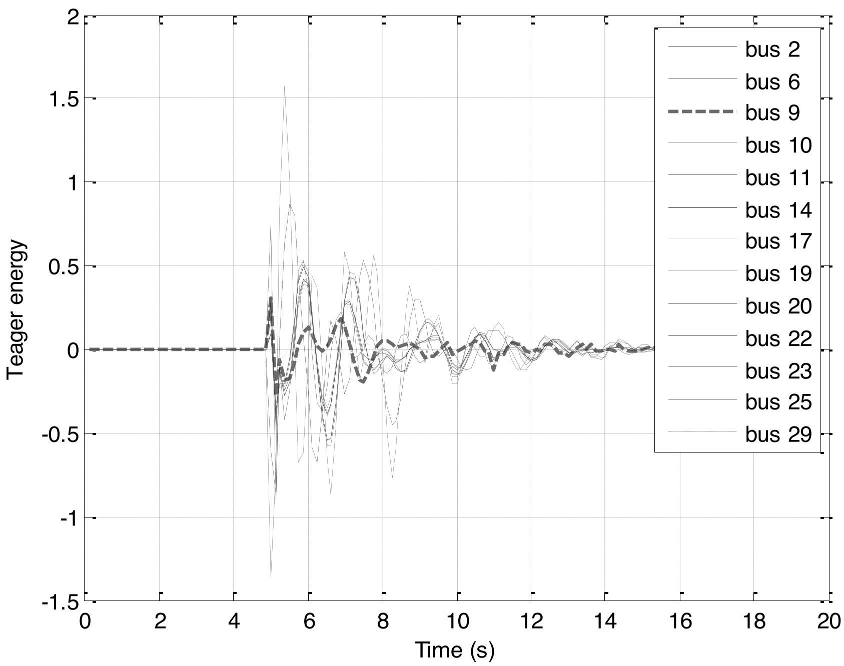

Fig. 8. TE of frequency signals for 2-25 TLO.

In this simulation (simulation of 2-25 TLO), all three applied signal processing techniques (DWT, HHT, and TEO) performed correct fault localization and identification, indicating bus 25 as fault location and time near 5 seconds as fault time, in the simulated outage of transmission line between buses 2 and 25. The complete comparison of the applied techniques is made according to the results of all simulations and presented in the next section.

The fault classification task is obtained with ANN, testing different structures of input and output patterns. Output data from the optimally used algorithms for fault identification and localization is input data for ANN (Fig. 9).

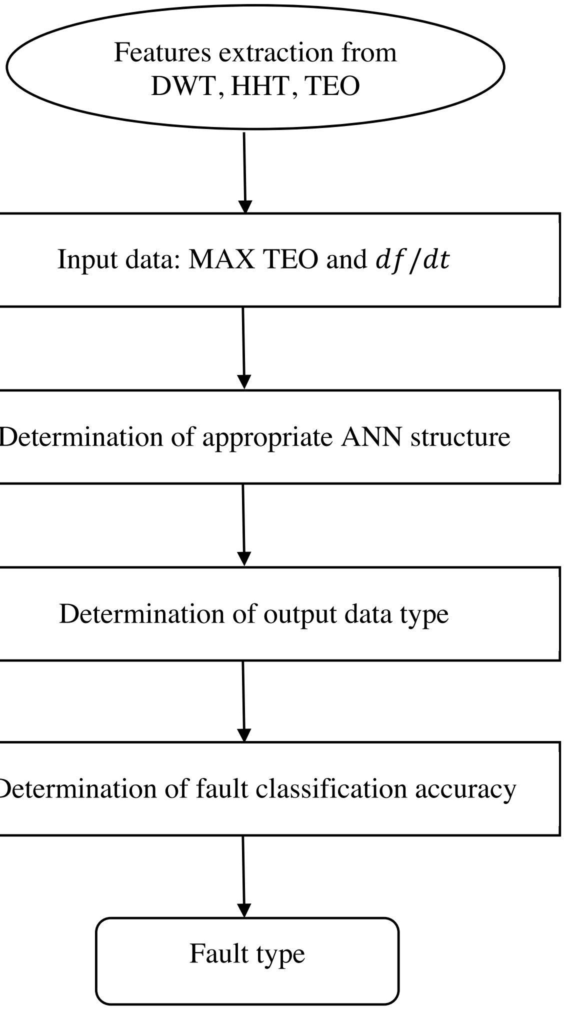

Fig. 9. Proposed approach for the fault classification with ANN.

RESULTS AND DISCUSSION

Fault identification and fault localization of the following fault types generator outage, transmission line outage, short circuit, and short circuit followed by adjacent transmission line outage are performed. Faults are simulated in DIgSILENT Power Factory NE39 bus test system – 111 faults totally (10 generator outage, 34 transmission line outage, 37 short circuits, 30 short circuits followed by adjacent transmission line outage). Simulated faults present symmetrical faults since all three phases are uniformly included in the event. Therefore, the short circuit simulations are performed as a three-phase short circuit. Simulations of the outages are performed as switch events (all three phases become open). In the short circuit followed by transmission line outage, transmission line outage is performed at the same time when a short circuit is cleared, uniformly for all phases. Frequency and voltage signals are obtained from 13 measurement points marked as the possible PMUs (phasor measurement units) in the system. The signals are then analyzed with DWT, HHT, and TEO. Fault time and fault location are specified as the results of the analysis. Frequency signals in the case of the generator and transmission line outage are analyzed in (Čišija-Kobilica et al., 2017). This paper is an extension of the previous research with results of the analysis included in this paper (marked italic in Table 1) so that complete comparison between different techniques, fault types, and signal types can be made.

Fault identification

Techniques comparison in the fault identification is based on RMSE (Root Mean Square Error), calculated with real fault time and fault time obtained by a specific technique as

$$\mathrm{RMSE}\ (\mathrm{x},\mathrm{y}) = \sqrt{\frac{1}{\mathrm{N}}\sum_{\mathrm{i}=1}^{\mathrm{N}}(\mathrm{x_i}-\mathrm{y_i})^2} \tag{8}$$

(x – real fault time of 0.5s, y – obtained fault time, N – the number of simulated faults) (Wang et al., 2009).

RMSE presents the average difference between real and predicted fault time (the deviation from the real time of the fault). In the fault identification part, RMSE values are determined using the results achieved with DWT, HHT, and TEO, for all cases in terms of fault time (Table 1).

Table 1. Fault identification results - RMSE values.

RMSE	**DWT results**		**TEO results**		**HHT results**	
Fault type/variable	Frequency	Voltage	Frequency	Voltage	Frequency	Voltage
Generator outage	*0.125s*	0	*0.125s*	0.068s	NO IMF	1.372s
TLO	0.121s	0	*0.109s*	0.091s	1.005s	0.66s
Short circuit	0.172s	0	0.174s	0.054s	0.787s	2.73s
Short circuit followed by TLO	0.163s	0	0.163s	0.076s	1.479s	2.576s

RMSE values are listed in Table 1 in order to highlight the technique that gives the best identification result for the specific fault types. If the comparison is made for the frequency signals analysis, TEO technique gives the best result in the case of the transmission line outage while DWT results are the best for the case of the short circuit fault type. Results for the generator outage and the short circuit followed by the transmission line outage are the same for the DWT and TEO technique, and better than the HHT results. In the voltage signals analysis, DWT has the best performance among applied techniques since all faults are correctly identified (RMSE equal to zero). RMSE values for the TEO application are not zero but very close to zero. Further, the comparison is performed between types of the analyzed signals, individually for each technique.

In the DWT analysis of the frequency signals, the best fault identification is performed in the case of the transmission line outage (the lowest deviation from the real fault time). Zero RMSE values (completely correct fault identification) for all fault types in the voltage signals analysis indicate the better fault identification performance than in the case of the frequency signals analysis.

RMSE values in the TEO analysis of the voltage signals are lower than RMSE values in the frequency signals analysis. Therefore, better fault identification results are achieved with voltage signals analysis rather than frequency signals analysis, in all cases with DWT and TEO application. As in the case of DWT analysis of the frequency signals, the best identification is performed in the case of the transmission line outage while short circuit simulations give the largest deviation of the exact fault time. The situation is reversed in the voltage signal analysis.

IMFs of the frequency signals are not obtained in the case of generator outage. The reason is that EMD is possible to apply for signals that have at least one maximum and one minimum and analyzed frequency signals for this fault type have the form of monotonic functions (Fig. 10). Since these signals in this case do not satisfy the mentioned condition further HHT could not be performed.

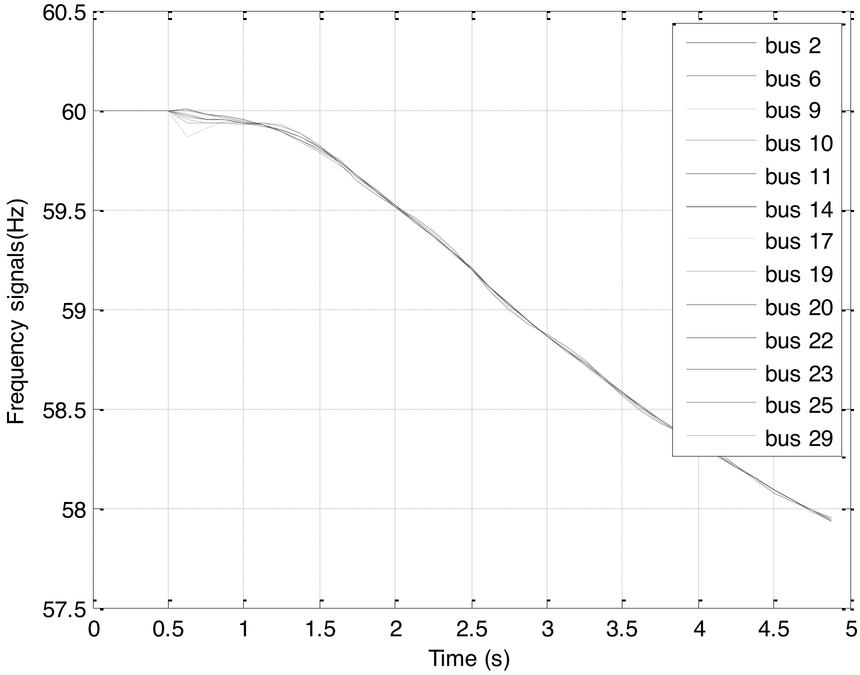

Fig. 10. Frequency signals in the case of generator outage fault type.

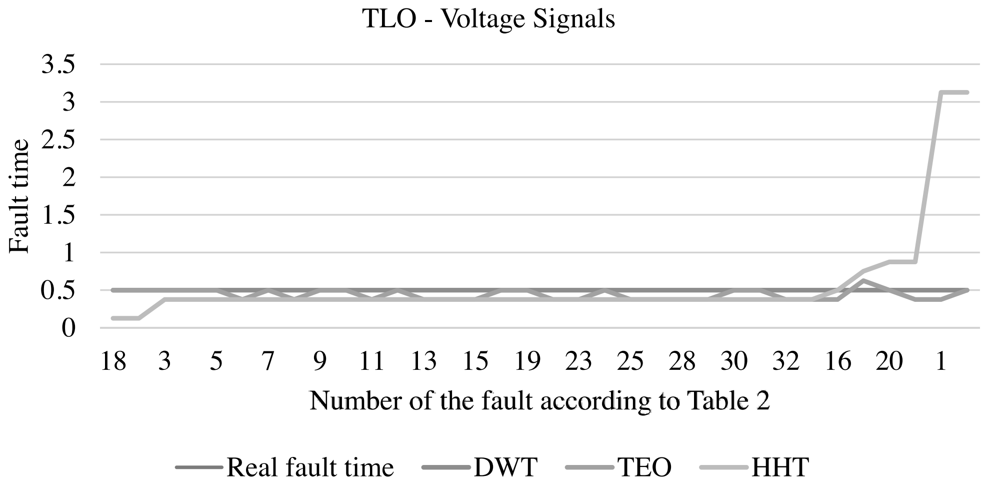

Fig. 11. Fault time for transmission line outage – voltage signals.

Very large deviation from correct fault identification is noticed for short circuit fault type and short circuit followed by transmission line outage, in terms of HHT technique. For other fault types, RMSE values are lower but still very big in comparison with the RMSE values of the other two techniques. Significant deviation of the results obtained with HHT analysis of voltage signals, for the case of transmission line outage, is graphically presented in Fig. 11.

Application of the TEO for the fault identification task provides satisfactory results that are very close to the most efficient results achieved with DWT technique, and much better than HHT results.

Fault localization

Accuracy (%) of the proposed techniques in the fault localization is determined in terms of the number of correctly located faults and total simulated faults. Applied criteria state that fault location is marked as correct if it is the nearest, second nearest, or adjacent measurement bus to the actual points where the fault occurred. The nearest buses are specified according to the transmission line lengths (other line parameters are not taken into consideration). Adjacent buses are not necessarily one of the nearest buses in terms of the line distance. Several fault results will explain the defined criteria. Results of TLO fault type in terms of voltage signals analysis are presented in Table 2.

Table 2. TLO at 0.5s (Voltage signals).

	Simulation	Fault Location		
No.	Fault location (buses)	DWT	TEO	HHT
1	1-2	29	25	29
2	1-39	29	2	29
3	9-39	9	9	9
4	8-9	6	6	6
5	5-8	29	9	9
6	7-8	29	9	6
7	6-7	29	9	9
8	5-6	6	14	14
9	4-5	6	14	17
10	3-4	6	6	6
11	4-14	14	6	6
12	2-3	14	14	14
13	2-25	25	25	25
14	13-14	10	14	6
15	10-13	10	14	14
16	10-11	10	11	11
17	6-11	11	11	6
18	14-15	14	14	14
19	15-16	14	14	10
20	16-17	29	29	22
21	16-19	29	19	23
22	16-21	22	22	22
23	16-24	23	23	17
24	17-18	23	17	14
25	17-27	29	17	17
26	3-18	29	2	17
27	21-22	22	17	23
28	22-23	23	23	23
29	23-24	23	17	17
30	25-26	29	29	29
31	26-27	29	29	17
32	26-29	29	29	29
33	26-28	29	29	29
34	28-29	29	29	29

a.) For the fault number 11 (transmission line 4-14), bus 14 in DWT analysis is marked as correct fault location, as it is the nearest measurement point to the location of the simulated fault,

b.) For the fault number 11, bus 6 in TEO and HHT analysis is also marked as correct fault location as it is second nearest measurement point to the location of the simulated fault,

c.) For the fault number 19 (transmission line 15-16), bus 14 (both, DWT and TEO analysis) is marked as correct fault location. It is not one of the nearest buses in terms of line distance (86.09475 km from the bus 15). The nearest buses are bus 17 (at 35.31075 km from bus 16) and bus 19 (at 77.36625 km from bus 16). Bus 14 is marked as correct fault location as it is adjacent bus to bus 15 (the bus that is included in simulated fault).

Accuracy values for the applied techniques in fault localization task are given below (Table 3).

Table 3. Fault localization results - accuracy (%).

Accuracy (%)	**DWT results**		**TEO results**		**HHT results**	
Fault type/variable	Frequency signals	Voltage signals	Frequency signals	Voltage signals	Frequency signals	Voltage signals
Generator outage	80	60	100	90	NO IMF	70
TLO	67.65	64.71	94.12	82.35	73.53	64.71
Short circuit	51.35	100	78.38	100	62.16	94.59
Short circuit followed by TLO	56.67	100	76.67	100	56.67	86.67

In the DWT and TEO analysis of the frequency signals, the best fault localization is performed in the case of the generator outage. The completely correct localization of short circuit and short circuit followed by TLO faults is performed in the voltage signals analysis, for both, DWT and TEO techniques.

The fault localization task in the HHT analysis of frequency signals has the highest accuracy for the TLO and the lowest for the SC followed by TLO fault type. In terms of the voltage signals analysis, the most efficient localization is performed in the case of SC.

When results are compared in terms of the analyzed signal (frequency or voltage) for all applications, better results in short circuit and SC followed by TLO are achieved with voltage signals analysis. For the generator outage and TLO, better results are provided when frequency signals are used in the analysis. What is mentioned is physically justified since frequency is related to the active power and consumption balance. Further, better results in the case of the short circuits fault types in the analysis of the voltage signals are justified with the physical relationship between reactive power and voltage during the disturbance.

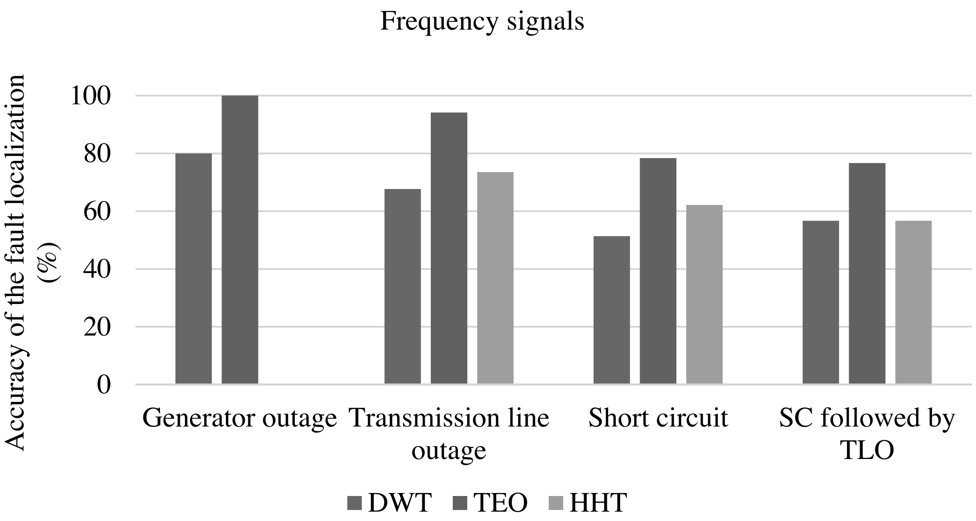

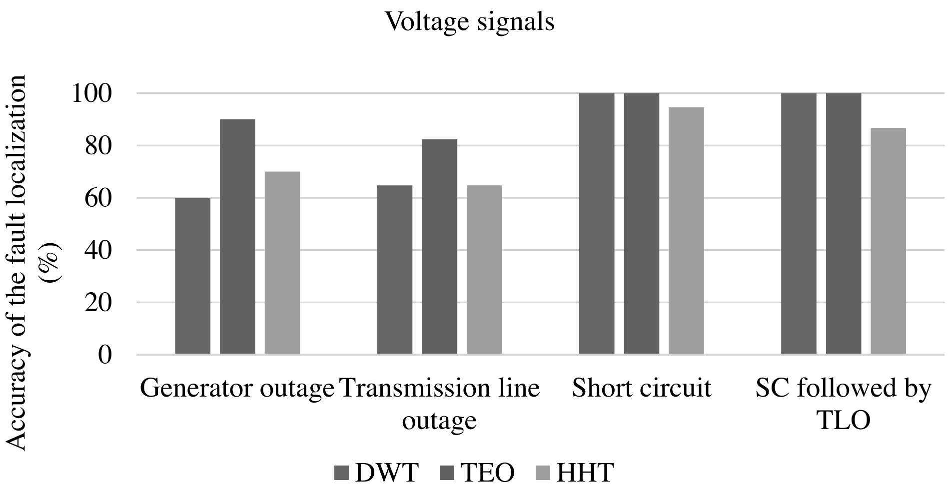

Fig. 12. Graphical representation of the obtained results.

Graphical representation of the obtained results with the applied techniques, concerning the type of the signal that has been analyzed, is shown with the following charts (Fig. 12).

The comparison made between techniques implicates that TEO provides better or same results in the fault localization for all fault types, in both, voltage and frequency signals analysis.

Fault classification

Various researchers identified that there is potential to use artificial neural networks (ANN) for the identification and classification tasks (Čišija-Kobilica et al., 2017). The fault classification task in this paper is obtained with testing of ANN with different structures of input, hidden, and output layers patterns. Output data possible to be extracted from the optimal algorithms for the fault identification and localization is used as input data for ANN. Different ANN structures are designed in order to correctly classify several fault types in the power system (C1 – generator outage, C2 – transmission line outage, C3 – three-phase short circuit (TPSC), C4 – three-phase short circuit followed by line outage, and C5 – TPSC followed by line outage and unsuccessful reclosing). This multiclassification task is performed with the pattern recognition neural network included in MATLAB. Simulations of the C5 fault type are performed in order to make a comparison of the achieved results with the results obtained in (Avdaković et al., 2014), where the same fault classification task is conducted. Totally 30 fault simulations are made for the C5.

Structures of the different input pattern, tested in the classification tasks, differ in the type and numbers of input variables. Two hidden layers are designed for all tested ANN structures with the difference made in the number of neurons in both of the hidden layers. Output data is fault type, and the number of the output variables, in terms of the number of the classified faults, was changing through the research in order to show how accuracy of the achieved classification results differ when classification of three (C1, C2, C3), four (C1, C2, C3, C4), or all five fault types (C1, C2, C3, C4, C5) is obtained. Classification of just three fault types (three output variables) is marked as reduced classification further in the paper. Four fault types classification (four output variables) is named initial classification while the term extended classification (five output variables) is used for the classification of all five simulated fault types.

The low-frequency component of the frequency signals can estimate the rate of change of weighted average frequency (frequency of the center of inertia) (Avdaković et al., 2014). DWT approximation coefficient at fifth level (A5) applied to the frequency signals has been successfully used in (Avdaković et al., 2011) for estimation of the parameter df/dt (rate of change of frequency). This component represents a direct power imbalance indicator (Avdaković et al., 2012); thus it can be included in the fault classification process. Component df/dt is included in the classification process obtained in this work in terms of the average frequency derivative (average value of A5 derivative).

Reduced and initial classification

This input data pattern is extracted from DWT and TEO analysis of the frequency and voltage signals obtained from five buses in the test system (buses 9, 17, 20, 23, and 25). The first extracted feature is in the form of maximum TE of the analyzed frequency signals. A derivative of the approximation coefficient from the fifth DWT decomposition level (A5) is computed for each sample of frequency signals. Average value of this variable presents the second extracted feature for the ANN structure (df/dt). The third extracted feature is maximum TE of analyzed voltage signals. The designed input pattern is tested with three and four output variables, thus performing initial and reduced classification. Train data is composed of 78 and 57 values, and the network is tested on the 33 and 24 values of each input variable for initial classification and reduced classification, respectively.

Separate ANN input data is formed from the extracted features in ANN structure 1 (Table 4). Maximum TE of frequency signals and mean of A5 derivatives present first ANN input set. Number of input variables is 10 (5 x max TE, 5 x df/dt). The highest classification accuracy of 78.79%, in initial classification, is obtained for the hidden layers in the form [10 5] and 95.83% in the form [7 6] for the reduced classification. The reason for the lower accuracy of the four fault types classification is related to the fault types C3 and C4. The unsuccessful distinction is made between these two fault types because of their similar fault nature. All generator and transmission line outages (C1 and C2) are correctly classified. The classifier can successfully classify the first three types of the fault with an accuracy of 95.83%.

Maximum TE of voltage signals as the third extracted feature is tested as a second separate data set (Table 4). The number of input variables is 5 (5 x max TE). Achieved classification accuracy when maximum TE of voltage signals is taken as ANN input variable is lower than in the case of first input data set for both initial and reduced classification, 75.76% and 87.5%, respectively. ANN with second input set shows very low accuracy in classification of C1 and C4. The similarity between C3 and C4 presents a reason for the unsuccessful classification of C4 fault type (33.33%). Fault types in terms of C2 and C3 are correctly classified. This classifier structure can successfully classify the first three types of the fault with an accuracy of 87.5%.

Table 4. Classification results in initial and reduced classification – accuracy (%).

Structure of ANN	ANN structure 1		ANN structure 2
Input data set	Frequency signals MAX TE, df/dt	Voltage signals MAX TE	Frequency signals MAX TE, df/dt, voltage signals MAX TE
Initial classification	78.79	75.76	84.85
Reduced classification	95.83	87.5	95.83

In ANN structure 2, extracted features are used as common ANN input data in order to show how the results change if all three variables present one input data set (Table 4). The number of input variables is 15. There is an improvement in achieved classification accuracy when compared with the case when the variables are taken as separate input to the ANN. The highest classification accuracy of 84.85% in initial classification is obtained for the hidden layers in the form [10 5] and 95.83% in the form [7 4] for the reduced classification. Classification accuracy, individually by each fault type, has satisfactory value for all cases.

Designed ANN structure is tested by reducing the number of the input variables from 15 to 9 variables. Mentioned variables reduction is accomplished by extracting the features from the frequency and voltage signals obtained at three buses (buses 9, 17, and 20). Input data is presented in the form [3 x max TE of frequency signals, 3 x df/dt, 3 x max TE of voltage signals]. Classification accuracy is not improved in the initial classification while perfect classification (100%) is achieved for the reduced classification.

Extended classification

Different ANN structures are tested in order to design the network that will accurately classify five fault types simulated in the test system. Faults of the C5 fault type are simulated in 30 different cases. Tested structures differ in the input layer (number and type of input variables) and the hidden layer (number of neurons). Train data is composed of 99 values, and the network is tested on the 42 values of each input variable. Achieved accuracy values for the different ANN structures are listed further in the paper (Table 5).

Table 5. Classification results in extended classification.

Type of Input Variables	Frequency signals MAX TE, df/dt			Voltage signals MAX TE			Frequency signals MAX TE, df/dt, voltage signals MAX TE		
Number of Input Variables	10	6	4	5	3	2	15	9	6
Number of neurons in hidden layers	[6 5]	[8 6]	[10 5]	[7 4]	[8 5]	[7 6]	[6 5]	[6 5]	[6 5]
Accuracy (%)	64.28	61.9	69.05	59.52	64.28	61.9	64.28	73.8	80.95

Improvement in the classification accuracy is achieved by reducing the number of the input variables. The classification results with the highest accuracy value of 80.95% are presented in detail, according to individual fault types (Table 6).

Table 6. Individual classification results.

Classes	C1	C2	C3	C4	C5	%
C1	2	1	0	0	0	66.67
C2	0	10	0	0	0	100
C3	0	0	9	1	1	81.82
C4	0	0	2	7	0	77.78
C5	0	0	2	1	6	66.67

Results are then compared with the results achieved in (Avdaković et al., 2014) where the same classification but with different input variables is performed. Achieved classification accuracy with the same wavelet function used (db4) was 80%, that is, slightly increased in this paper. Improvements are noticed for the classification of fault types C2 and C3, while lower accuracy values are obtained for another fault types, when results are compared by individual accuracy values in fault types. The improvement achieved in this work is presented with the result that individual classification accuracy is higher than 66% for all classes.

CONCLUSION

In this paper, a new approach for the identification, localization, and classification of the disturbances in the power system is proposed. The proposed approach is based on the application of the advanced signal processing techniques (TEO, DWT, and HHT) and availability of PMUs signals in the Wide-Area Monitoring, Protection and Control Systems (WAMPAC). Performed analyses show that the proposed approach gives good results with the possibility of the further improvement. The reality of the existing power systems is the development of the smart systems that brings a challenge for the scientific and professional community in making adequate approaches.

With the represented analyses, it can be concluded that analysis of the frequency signals (including df/dt parameter as the classifier input) gives better results in the case of the generator outage fault type. What is mentioned is physically justified since frequency is related to the active power and consumption balance. Further, analysis of the voltage signals provides better results in the case of the short circuits fault types what is related to the physical relationship between reactive power and voltage during the disturbance.

Completeness of the fault detection work is achieved with a complete, accurate, and fast algorithm for the fault identification, localization, and classification. The novelty of the work is found in the application of TEO for the complete fault detection (fault identification, localization, and classification) of specific fault types, with the satisfactory results achieved. The comparison made between applied techniques implicates that TEO provides better or same results in the fault detection, for all fault types, in both voltage and frequency signals analysis. With less computational work required, a technique with TEO application could be a base for the development of a relatively simple algorithm for the identification, localization, and classification of the disturbances in the power system.

Finally, the proposed approach, with the availability of signals obtained from the PMUs and required communication infrastructure, could be a good foundation for the development of the algorithms for fast and effective identification, localization, and classification of the disturbances, and eventually development of the adaptive under frequency protection.

REFERENCE

Avdakovic, S., Becirovic, E., Nuhanovic, A. & Kusljugic, M. 2014. Generator Coherency Using the Wavelet Phase Difference Approach. IEEE Transactions on Power Systems **29**(1): 271-278.

Avdaković, S., Nuhanović, A. & Kušljugić. 2011. An Estimation Rate of Change of Frequency Using Wavelet Transform. International Review of Automatic Control (I.RE.A.CO.) **4**(2): 267-272.

Avdaković, S., Nuhanović, A., Kušljugić, M. & Bećirović, E. 2014. Applications of wavelets and neural networks for classification of power system dynamic events. Turkish Journal of Electrical Engineering & Computer Sciences **22**(2): 327-340.

Avdaković, S., Nuhanović, A., Kušljugić, M. & Musić, M. 2012. Wavelet transform applications in power system dynamics. Electric Power Systems Research **83**(1): 237-245.

Chakrabortty, A. & Khargonekar, P. P. 2013. Introduction to Wide-Area Control of Power Systems. American Control Conference (ACC). Washington.

Chen, Z. M., Li, M. S., Ji, T. Y. & H., W. Q. 2016. Detection and Classification of Power Quality Disturbances in Time Domain Using Probabilistic Neural Network. Neural Networks (IJCNN), 2016 International Joint Conference on. Vancouver.

Čišija-Kobilica, N. & Avdaković, S. 2017. Application of Teager Energy Operator for the Power System Fault Identification and Localisation. International Symposium on Innovative and Interdisciplinary Applications of Advanced Technologies: 18-29. Springer, Cham.

Čišija-Kobilica, N. & Avdaković, S. 2017. Fault Classification with Artificial Neural Networks based on the Application of Teager Energy Operator. International Journal of Engineering Research and Development **13**(11): 31-36.

Daubechies, I. 1992. Ten Lectures on Wavelet. Philadelphia: Society for Industrial and Applied Mathematics (SIAM).

Grigsby, L. L. 2007. Power System Stability and Control. New York: Taylor and Francis Group.

Hasheminejad, S., Ghodratollah Seifossadat, S. & Joorabian, M. 2017. New travelling-wave-based protection algorithm for parallel transmission lines during inter-circuit faults. IET Generation, Transmission & Distribution **11**(6): 3984-3991.

Hasheminejad, S., Seifossadat, S. G., Razaz, M. & Joorabian, M. 2016. Traveling-wave-based protection of parallel transmission lines using Teager energy operator and fuzzy systems. IET Generation, Transmission & Distribution **10**(4): 1067-1074.

Hayes, B. & Condon, M. 2016. Application of the Real-Time Hilbert Huang Transform to a Noise Perturbed Buck Converter. 10th International Conference on Circuits, Systems, Signal and Telecommunications (CSST '16). Barcelona.

Hongbo, W., Rong, H., Qi, Q. & Yu, K. 2014. Improved Teager Energy Operator for On-Line Tracking of Power Grid Voltage. 33rd Chinese Control Conference. Nanjing.

Ivatloo, B. M. 2009. Optimal Placement of PMUs for Power System Observability Using Topology Based Formulated Algorithms. Journal of Applied Science **9**(13): 2463-2468.

Kaiser, J. F. 1990. On a simple algorithm to calculate the 'energy' of a signal. Acoustics, Speech, and Signal Processing, 1990. ICASSP-90., 1990 International Conference on. Albuquerque.

Kamwa, I., Pradhan, A. K. & Joos, G. 2011. Robust Detection and Analysis of Power System Oscillations Using the Teager-Kaiser Energy Operator. IEEE Transactions on Power Systems **26**(1): 323-333.

Kumar, J. & Jena, P. 2016. Fault Detection during Power Swing using Teager-Kaiser Energy Operator. Power Systems (ICPS), 2016 IEEE 6th International Conference on. New Delhi.

Lee, J.-W., Kim, W.-K., Han, J., Jang, W.-H. & Kim, C.-H. 2016. Fault Area Estimation Using Traveling Wave for Wide Area Protection. J. Mod. Power Syst. Clean Energy **4**(3): 478 - 486.

Li, F., Gao, Y., Cao, Y. & Iravani, R. 2016. Improved Teager Energy Operator and Improved Chirp-Z Transform for Parameter Estimation of Voltage Flicker. IEEE Transactions on Power Delivery **31**(1): 245-253.

Mallat, S. 1998. A Wavelet Tour of Signal Processing. Michigan: Academic Press.

Maragos, P., Kaiser, J. F. & Quatieri, T. F. 1993. Energy Separation in Signal Modulations with Application to Speech Analysis. IEEE Transactions on Signal Processing **41**(10): 3024-3051.

Messina, A. 2009. Inter-Area Oscillations in Power Systems: A Nonlinear and Nonstationary Perspective. Springer Science & Business Media.

Muller, S. C., Kubis, A., Brato, S., Hager, U., Rehtanz, C. & Gotze, J. 2012. New Applications for Wide-Area Monitoring, Protection and Control. 3rd IEEE PES Innovative Smart Grid Technologies Europe (ISGT Europe). Berlin.

Neto, C. M., Costa, F. B., Barreto, R. L., Rocha, T. O. & Ribeiro, R. L. 2013. Wavelet-Based Method for Detection of Electrical and Electromechanical Oscillations in Synchronous Generators. Power Electronics Conference (COBEP), 2013 Brazilian. Gramado.

Prasertwong, K., Mithulananthan, N. & Thakur, D. 2010. Understanding low-frequency oscillation in power systems. International Journal of Electrical Engineering Education **47**(3): 248-262.

Ramakrishna, G. & Padmaja, N. 2016. Estimation of Teager Energy Using EMD and HHT. Applied and Theoretical Computing and Communication Technology (iCATccT), 2016 2nd International Conference on. Bangalore.

Reddy, M. B., Rajesh, V., Gopakumar, P. & Mohanta, D. K. 2014. Smart Fault Location for Smart Grid Operation Using RTUs and Computational Intelligence Techniques. IEEE Systems Journal **8**(4): 1260-1271.

Reza, M., Ciobotaru, M. & Agelidis, V. G. 2015. Single-Phase Grid Voltage Frequency Estimation Using Teager Energy Operator-Based Technique. IEEE Journal of Emerging and Selected Topics in Power Electronics **3**(4): 1218-1227.

Rueda, J. L., Juarez, C. A. & Erlich, I. 2011. Wavelet-Based Analysis of Power System Low-Frequency Electromechanical Oscillations. IEEE Transactions on Power Systems **26**(3): 1733-1743.

Wall, P., Dattaray, P., Jin, Z., Mohapatra, P., Yu, J., Wilson, D., . . . Terzija, V. 2016. Deployment and Demonstration of Wide Area Monitoring System in Power System of Great Britain. J. Mod. Power Syst. Clean Energy **4**(3): 506-518.

Wang, Z. & Bovik, A. C. 2009. Mean Squared Error: Love It or Leave It? A new look at signal fidelity measures. IEEE Signal Processing Magazine **26**(1): 98-117.

Xiao, H., Wei, J., Liu, H., Li, Q., Shi, Y. & Zhang, T. 2017. Identification method for power system low-frequency oscillations based on improved VMD and Teager–Kaiser energy operator. IET Generation, Transmission & Distribution **11**(16): 4096-4103.

Yao, W., Teng, Z., Tang, Q. & Gao, Y. 2016. Measurement of power system harmonic based on adaptive Kaiser self-convolution window. IET Generation, Transmission & Distribution **10**(2): 390-398.

Yin, S., Hu, N. & Hu, L. 2015. Teager Energy Operator and its Application in the Study of Induction Motor Rotor Broken Bars Fault. Prognostics and System Health Management Conference. Beijing.

Zhang, Y., Wang, Z. & Zhang, J. 2012. Bayesian Fault Detection Based on WAMS/PMU Measurement System. Power and Energy Society General Meeting, 2012 IEEE. San Diego.

Submitted: 07/03/2018
Revised: 10/07/2018
Accepted: 30/09/2018

طريقة جديدة لتحديد أخطاء نظام الطاقة وتوطينها وتصنيفها

نيرى تشيشيبا–كوبيليتسا، **سامر أوداكوفيتش، *ياسنى حفظي أفأنديتش وأرمين كوبيليتسا**
*قسم الهندسة الكهربائية والالكترونية، جامعة بورش الدولية، سراييفو، البوسنة والهرسك
**الشركة البوسنية للكهرباء، سراييفو، البوسنة والهرسك
***قسم المعلومات وعلوم الحاسب، جامعة الملك فهد للبترول والمعادن، الظهران، المملكة العربية السعودية

الخلاصة

يتضمن الهيكل الحديث لمراقبة أنظمة الطاقة وحمايتها والتحكم فيها وحدات القياس المتزامنة مع نظام تحديد المواقع العالمي GPS (وحدات قياس فاسور). مع تنفيذ هذه الوحدات، يلزم توافر المراقبة على نطاق واسع وأنظمة الحماية والتحكم لإجراء تحديد سريع وفعال للاضطرابات التي قد تؤدي إلى الانتشار المتتالي وانقطاع التيار الكهربائي في نظام الطاقة. وعلاوة على ذلك، تُمكّن المتطلبات من اتخاذ إجراءات مناسبة وتدابير وقائية وتصحيحية لتقليل آثار الاضطرابات التي حدثت. يقترح هذا البحث تطبيق مشغل الطاقة تيجر (تيو) من أجل تحديد أخطاء نظام الطاقة، وتوطينها، وتصنيفها. يتم تحديد وتعيين الاضطرابات من تحليل الإشارات المتاحة مع تطبيق مشغل الطاقة تيجر، ومقارنة قيم الذروة في عدة نقاط في النظام. ويستند التصنيف المقترح للاضطرابات إلى تحليل مشغل الطاقة تيجر للإشارات والقيم المتاحة لمؤشر دي تي / دي أف لاختلال توازن القوى النشطة في عدة نقاط في النظام. يتم إجراء عمليات المحاكاة في نظام اختبار ناقل نيو أنجيلاند 39 باستخدام برنامج ديجيسيلنت. يتم تقييم الأداء والمقارنة بين التقنيات المُطبقة من خلال عدد كبير من أخطاء المحاكاة لنوع الصدع المُحدد. تتم مقارنة نتائج تحديد الأعطال والتوطين مع النتائج التي تم الحصول عليها في التحليل الذي تم إجراؤه مع تحويل المويجات المنفصلة وتحويل هيلبرت–هوانغ مما يشير إلى الأداء المرضي للنهج المقترح. علاوة على ذلك، يوفر النهج المُقترح نتائج ملحوظة في تصنيف الخطأ الذي تم إجراؤه وفقاً لـ 141 من عيوب المحاكاة. ويتفوق مشغل الطاقة تيجر في الطريقة المُقترحة على التقنيات الأخرى مع ذات العمل الحسابي الأقل والتقدير الأسرع، مما يسمح بتطوير خوارزمية بسيطة نسبياً لتحديد سريع وفعال وتصنيف الاضطرابات في نظام الطاقة.